

## ARTICLE

# Temperature-controlled Structural Diversity of Two Cd(II) Coordination Polymers Based on the Dicarboxylate Ligand<sup>①</sup>

CHEN Fang-Min<sup>a</sup> ZHOU Chi-Chi<sup>a</sup> HE Xiong<sup>a</sup>LI Yan<sup>a②</sup> ZHANG Xiu-Qing<sup>a②</sup>

<sup>a</sup>(College of Chemistry and Bioengineering, Guangxi Key Laboratory of Electrochemical and Magnetochemical Functional Materials, Guilin University of Technology, Guilin 541004, China)

**ABSTRACT** Two new 3-D Cd(II) coordination polymers with *p*-phthalic acid (*p*-BDC) and 4,4'-dipyridyl-amine (4,4'-dpa), namely  $[\text{Cd}_2(\text{p-BDC})_2(4,4'\text{-dpa})_2]_n$  **1** and  $\{[\text{Cd}(\text{p-BDC})(4,4'\text{-dpa})(\text{H}_2\text{O})]\cdot 4\text{H}_2\text{O}\}_n$  **2** were successfully synthesized under hydrothermal conditions at 120 and 140 °C. They were characterized by single-crystal X-ray diffraction, IR, PXRD and TGA. It was further characterized by Hirshfeld surface (HS) analysis for complex **2**. The luminescent properties of the complexes have also been investigated.

**Keywords:** Cd(II) coordination polymers, *p*-phthalic acid, Hirshfeld surface, Luminescent properties;

**DOI:** 10.14102/j.cnki.0254-5861.2011-3234

## 1 INTRODUCTION

Recently, the design of coordination polymers (CPs) has attracted considerable attention not only for their interesting topological structures<sup>[1]</sup> but also for their potential applications in the fields of magnetism, luminescence, gas adsorption, catalysis, electrical conductivity, and so on<sup>[2–5]</sup>. To date, how to rationally design and synthesize aiming metalorganic complexes with the expected structure and prospective properties is still a big challenge. Thereinto, selecting suitable ligands is crucially to construct complexes with special functionality. However, it remains difficult to predict the exact structures and control the construction of these CPs<sup>[6, 7]</sup> because they might be easily influenced by many factors, such as the geometry of organic ligands, coordination number of metal ions, solvents, pH value of the solution, reaction time, etc<sup>[8–11]</sup>. Apart from these factors, higher reaction temperature may lead to complicated structures due to the increase in connected number of ligands, the appearance of entanglement, hydroxo metal clusters and so on<sup>[12]</sup>. Due to different temperatures, a great number of these complexes possessing novel structures and interesting

properties have been effectively prepared under hydrothermal conditions. Inspired by the aforementioned considerations, two novel Cd(II) CPs based on *p*-phthalic acid and 4,4'-bipyridylamine ligand, namely,  $[\text{Cd}_2(\text{p-BDC})_2(4,4'\text{-dpa})_2]_n$  **1** and  $\{[\text{Cd}(\text{p-BDC})(4,4'\text{-dpa})(\text{H}_2\text{O})]\cdot 4\text{H}_2\text{O}\}_n$  **2**, have been successfully obtained under hydrothermal conditions at different temperature. Herein, we report the synthesis, crystal structures and luminescent properties of the polymers in this work.

## 2 EXPERIMENTAL

### 2.1 Materials and instruments

All chemicals for syntheses were commercially available (Aldrich, Aladdin, Alfa Aesar or Xilong Scientific) and used as received without further purification. The structures of the complexes have also been confirmed by single-crystal X-ray (Agilent G8910A CCD) diffraction analyses. The Fourier transform infrared spectra were recorded using KBr pellets ranging from 4000 to 500 cm<sup>-1</sup> on a PerkinElmer spectrum one FT-IR spectrometer. Powder X-ray diffraction (XRD) data were collected on a Bruker D8 Advance X-ray diffracto-

Received 25 April 2021; accepted 29 June 2021 (CCDC 1446321 and 1478443)

① This work was supported by the Foundation of Guangxi Key Laboratory of Electrochemical and Magneto-chemical Functional Materials (EMFM20161102) and the National Natural Science Foundation of China (No. 61765005)

② Corresponding authors. Zhang Xiu-Qing, born in 1979, associate professor. E-mail: glutchem@163.com; Li Yan, E-mail: ly741110@163.com

meter with  $\text{CuK}\alpha$  radiation ( $\lambda = 1.5418 \text{ \AA}$ ). The thermal behavior was carried out by a SDTQ 600 apparatus. The photoluminescence spectra for the solid samples were measured at room temperature on a RF-4600 fluorescence spectrophotometer.

## 2.2 Preparation of $[\text{Cd}_2(p\text{-BDC})_2(4,4'\text{-dpa})_2]_n$ **1**

A mixture of  $\text{Cd}(\text{NO}_3)_2 \cdot 4\text{H}_2\text{O}$  (0.1542 g, 0.5 mmol),  $p\text{-BDC}$  (0.0831 g, 0.5 mmol),  $4,4'\text{-dpa}$  (0.0855 g, 0.5 mmol),  $\text{NaOH}$  (0.0400 g, 1 mmol), and  $\text{H}_2\text{O}$  (15 mL) was stirred at room temperature for 10 min. Then, it was sealed in a 25 mL Teflon-lined stainless-steel container. The mixture was heated at  $120^\circ\text{C}$  for 72 h. After slowly cooling to room temperature at a rate of  $10^\circ\text{C}\cdot\text{h}^{-1}$ , the mixture was washed with alcohol/distilled water and faint yellow lump-shaped crystals were filtered off and dried at room temperature (Yield: 0.077 g, 28% based on Cd). Anal. Calcd. (%) for  $\text{C}_{36}\text{H}_{26}\text{Cd}_2\text{N}_6\text{O}_8$  **1**: C, 48.24; H, 2.90; N, 9.38. Found (%): C, 48.21; H, 2.89; N, 9.34. IR ( $\text{cm}^{-1}$ , KBr): 3451 (m, O-H), 1562 (m, COO-), 1392 (m, COO-), 1210 (m, C-H), 1015 (m, C-H), 820 (m, N-M) 738 (m, O-M).

## 2.3 Preparation of $\{[\text{Cd}(p\text{-BDC})(4,4'\text{-dpa})(\text{H}_2\text{O})] \cdot 4\text{H}_2\text{O}\}_n$ **2**

A mixture of  $\text{Cd}(\text{NO}_3)_2 \cdot 4\text{H}_2\text{O}$  (0.1542 g, 0.5 mmol),  $p\text{-BDC}$  (0.0831 g, 0.5 mmol),  $4,4'\text{-dpa}$  (0.0855 g, 0.5 mmol),  $\text{NaOH}$  (0.0400 g, 1 mmol), and  $\text{H}_2\text{O}$  (15 mL) was stirred at room temperature for 10 min. Then, it was sealed in a 25 mL Teflon-lined stainless-steel container. The mixture was heated at  $140^\circ\text{C}$  for 72 h. After slowly cooling to room temperature

at a rate of  $10^\circ\text{C}\cdot\text{h}^{-1}$ , the mixture was washed with alcohol/distilled water and faint yellow lump-shaped crystals were filtered off and dried at room temperature (Yield: 0.042 g, 16% based on Cd). Anal. Calcd. (%) for  $\text{C}_{36}\text{H}_{46}\text{Cd}_2\text{N}_6\text{O}_{18}$  **2**: C, 40.16; H, 4.27; N, 7.81. Found (%): C, 40.13; H, 4.25; N, 7.79. IR ( $\text{cm}^{-1}$ , KBr): 3432 (m, O-H), 1566 (m, COO-), 1386 (m, COO-), 1216 (m, C-H), 1008 (m, C-H), 814 (m, N-M), 758 (m, O-M).

## 2.4 X-ray crystal structure determination

Single-crystal X-ray diffraction analyses of **1** and **2** were carried out on an Agilent Technologies G8910A CCD diffractometer equipped with graphite-monochromated  $\text{MoK}\alpha$  radiation ( $\lambda = 0.71073 \text{ \AA}$ ) using an  $\omega$ -scan mode. The  $\phi$ -scan technique was employed to measure intensities. Absorption corrections were applied empirically using the SADABS<sup>[13]</sup>. The crystal structures were solved by direct methods and difference Fourier synthesis and refined by full-matrix least-squares using SHELXL<sup>[13]</sup>. An absorption correction was applied based on the comparison of multiple symmetry equivalent measurements. The structures were solved by direct methods using SHELXS-97 and refined anisotropically by full-matrix least-squares methods on  $F^2$  using SHELXL-97 for all non-hydrogen atoms<sup>[15, 16]</sup>. Crystal data as well as details of data correction and refinement for complexes **1** and **2** are summarized in Table 1. Selected bond lengths and bond angles are listed in Tables 2 and 3, and H-bonds for **2** are listed in Table 4.

Table 1. Crystallographic Data and Details for **1** and **2**

Complexes	<b>1</b>	<b>2</b>
Formula	$\text{C}_{36}\text{H}_{26}\text{Cd}_2\text{N}_6\text{O}_8$	$\text{C}_{36}\text{H}_{46}\text{Cd}_2\text{N}_6\text{O}_{18}$
$M_r$	895.43	1075.59
Crystal system	Monoclinic	Orthorhombic
Space group	$P2_1/n$	$Pbca$
$a$ ( $\text{\AA}$ )	10.1682(5)	15.0032(7)
$b$ ( $\text{\AA}$ )	24.0865(11)	16.0105(8)
$c$ ( $\text{\AA}$ )	15.3011(7)	17.3857(8)
$\beta$ ( $^\circ$ )	103.080(5)	90
$V$ ( $\text{\AA}^3$ )	3650.2(3)	4176.2(3)
$Z$	4	4
$F(000)$	1776	2176
$\mu$ ( $\text{mm}^{-1}$ )	1.224	1.102
$\rho$ ( $\text{g}\cdot\text{cm}^{-3}$ )	1.629	1.711
$R^a, b_{\text{int}}$	0.0343	0.0256
$R$ ( $I > 2\sigma(I)$ )	$R = 0.0726$ , $wR = 0.1753$	$R = 0.0323$ , $wR = 0.0783$
$R$ (all data)	$R = 0.0919$ , $wR = 0.1829$	$R = 0.0455$ , $wR = 0.0909$
$Goof$	1.196	1.070
$(\Delta\rho)_{\text{max}}/(\Delta\rho)_{\text{min}}$ ( $\text{e}/\text{\AA}^3$ )	2.080 and -0.992	0.320 and -1.207

**Table 2.** Selected Bond Lengths (Å) and Bond Angles (°) for **1**

Bond	Dist.	Bond	Dist.	Bond	Dist.
Cd(1)–O(2)	2.341(7)	Cd(2)–O(1)	2.311(7)	Cd(1)–O(4A)	2.254(7)
Cd(1)–O(7B)	2.454(6)	Cd(2)–O(5)	2.251(7)	Cd(1)–O(8B)	2.344(7)
Cd(1)–N(3C)	2.268(8)	Cd(2)–N(4)	2.336(8)	Cd(1)–N(6D)	2.315(8)
Cd(2)–N(4)	2.336(8)	Cd(2)–O(3A)	2.216(7)	Cd(2)–N(1)	2.327(7)
Angle	(°)	Angle	(°)	Angle	(°)
O(2)–Cd(1)–O(7A)	104.9(2)	O(2)–Cd(1)–O(8A)	158.7(2)	O(1)–Cd(2)–N(4)	85.8(3)
O(4B)–Cd(1)–O(2)	114.5(3)	O(4B)–Cd(1)–O(7A)	136.5(3)	O(3B)–Cd(2)–O(5)	136.3(3)
O(4B)–Cd(1)–O(8A)	85.9(3)	O(4B)–Cd(1)–N(3C)	109.0(3)	O(3B)–Cd(2)–N(4)	87.5(3)
O(4B)–Cd(1)–N(6D)	85.9(3)	O(8A)–Cd(1)–O(7A)	53.8(2)	O(5)–Cd(2)–N(4)	89.3(3)
N(3C)–Cd(1)–O(2)	86.9(3)	N(3C)–Cd(1)–O(7A)	90.2(2)	N(1)–Cd(2)–N(4)	173.4(3)
N(3C)–Cd(1)–O(8A)	92.3(3)	N(3C)–Cd(1)–N(6D)	163.9(3)	O(3B)–Cd(2)–O(1)	130.9(3)
N(6D)–Cd(1)–O(2)	80.9(3)	N(6D)–Cd(1)–O(7A)	82.9(3)	O(3B)–Cd(2)–N(1)	96.9(3)
N(6D)–Cd(1)–O(8A)	95.2(3)	O(1)–Cd(2)–N(1)	94.9(3)	O(5)–Cd(2)–O(1)	92.2(3)
O(5)–Cd(2)–N(4)	89.3(3)				

Symmetry codes: <sup>A</sup>1 + *x*, *y*, *z*; <sup>B</sup>*x*, *y*, 1 + *z*; <sup>C</sup>1/2 – *x*, –1/2 + *y*, 3/2 – *z*; <sup>D</sup>1/2 – *x*, 1/2 + *y*, 3/2 – *z***Table 3.** Selected Bond Lengths (Å) and Bond Angles (°) for **2**

Bond	Dist.	Bond	Dist.	Bond	Dist.
Cd(1)–O(3)	2.385(2)	Cd(1)–O(4)	2.386(2)	Cd(1)–O(2)	2.266(2)
Cd(1)–N(1)	2.364(3)	Cd(1)–O(1)	2.580(2)	Cd(1)–N(3A)	2.303(3)
Cd(1)–O(5)	2.623(3)				
Angle	(°)	Angle	(°)	Angle	(°)
O(3)–Cd(1)–O(4)	54.88(8)	O(3)–Cd(1)–O(1)	80.19(8)	N(3A)–Cd(1)–O(3)	89.29(9)
O(3)–Cd(1)–O(5)	121.91(8)	O(4)–Cd(1)–O(1)	82.44(8)	N(3A)–Cd(1)–N(1)	88.98(9)
O(4)–Cd(1)–O(5)	77.95(9)	N(1)–Cd(1)–O(3)	103.35(9)	N(3A)–Cd(1)–O(5)	73.59(9)
N(1)–Cd(1)–O(4)	155.39(9)	N(1)–Cd(1)–O(1)	82.39(9)	N(3A)–Cd(1)–O(4)	100.93(9)
N(1)–Cd(1)–O(5)	126.63(10)	O(1)–Cd(1)–O(5)	121.91(8)	N(3A)–Cd(1)–O(1)	164.43(9)
O(2)–Cd(1)–O(3)	131.06(8)	O(2)–Cd(1)–O(4)	99.08(8)	O(2)–Cd(1)–O(5)	76.31(8)
O(2)–Cd(1)–N(1)	87.32(9)	O(2)–Cd(1)–O(1)	53.67(8)	O(2)–Cd(1)–N(3A)	139.15(9)

Symmetry code: <sup>A</sup>1 – *x*, 1/2 + *y*, 3/2 – *z***Table 4.** Hydrogen Bond Lengths (Å) and Bond Angles (°) for Complex **2**

D–H···A	D–H	H···A	D···A	D–H···A
O(9)–H(9A)···O(4) <sup>1</sup>	0.85	1.94	2.792(3)	175
O(9)–H(9B)···O(8)	0.85	2.02	2.835(3)	159
O(7)–H(7B)···O(2) <sup>1</sup>	0.85	2.00	2.840(3)	170
O(8)–H(8A)···O(3)	0.85	1.99	2.831(3)	172
O(8)–H(8B)···O(7) <sup>2</sup>	0.85	2.01	2.840(4)	163
O(6)–H(6A)···O(9) <sup>3</sup>	0.85	2.05	2.898(4)	174
O(6)–H(6B)···O(1)	0.85	2.02	2.872(4)	177

Symmetry codes: <sup>1</sup>1/2 – *x*, –1/2 + *y*, *z*; <sup>2</sup>*x*, –1/2 – *y*, –1/2 + *z*; <sup>3</sup>–1/2 + *x*, *y*, 3/2 – *z*

### 3 RESULTS AND DISCUSSION

#### 3.1 Crystal structure of [Cd<sub>2</sub>(*p*-BDC)<sub>2</sub>(4,4'-dpa)<sub>2</sub>]<sub>n</sub> **1**

Crystallographic analysis reveals that complex **1** crystallizes in the monoclinic system *P2<sub>1</sub>/n* space group. The asymmetric unit of complex **1** contains two Cd(II) cations, two 4,4'-dpa ligands and two *p*-BDC<sup>2–</sup> anions. The two Cd(II) ions lie in two different environments, as shown in Fig. 1a. The Cd(1) is six-coordinated by four oxygen atoms from

three *p*-BDC<sup>2–</sup> anions and two nitrogen atoms from two 4,4'-dpa ligands. The Cd(1)–O bond lengths vary from 2.253(2) to 2.464(2) Å, and the Cd(1)–N bond lengths change from 2.267(7) to 2.310(8) Å. Six atoms form a distorted octahedral coordination geometry. The Cd(2) is five-coordinated by three oxygen atoms from three *p*-BDC<sup>2–</sup> anions and two nitrogen atoms from two 4,4'-dpa ligands. The Cd(2)–O bond lengths vary from 2.215(6) to 2.310(6) Å, and the Cd(2)–N bond lengths change from 2.325(7) to

2.333(7) Å. The coordination geometry around the Cd(2) ion can be regarded as an intermediate between square pyramid and trigonal bipyramid as described by the  $\tau$  parameter of 0.61<sup>[17]</sup>. Two Cd(II) centers are bridged by carboxylate groups from two different  $\mu_4$ -*p*-BDC<sup>2-</sup> anions, generating a binuclear Cd<sub>2</sub> unit with a Cd···Cd distance of 4.005 Å.

Further linkage of these Cd<sub>2</sub> units via both  $\mu_3$ - and  $\mu_4$ -*p*-BDC<sup>2-</sup> moieties furnishes a 3D structure. The carboxylate groups of *p*-BDC<sup>2-</sup> blocks alternately bridge the adjacent Cd(II) ions to form a 2-D metal-organic net (Fig. 1b). The 2-D layers are further connected by 4,4'-dpa ligands to form a 3-D structure (Fig. 1c and 1d).

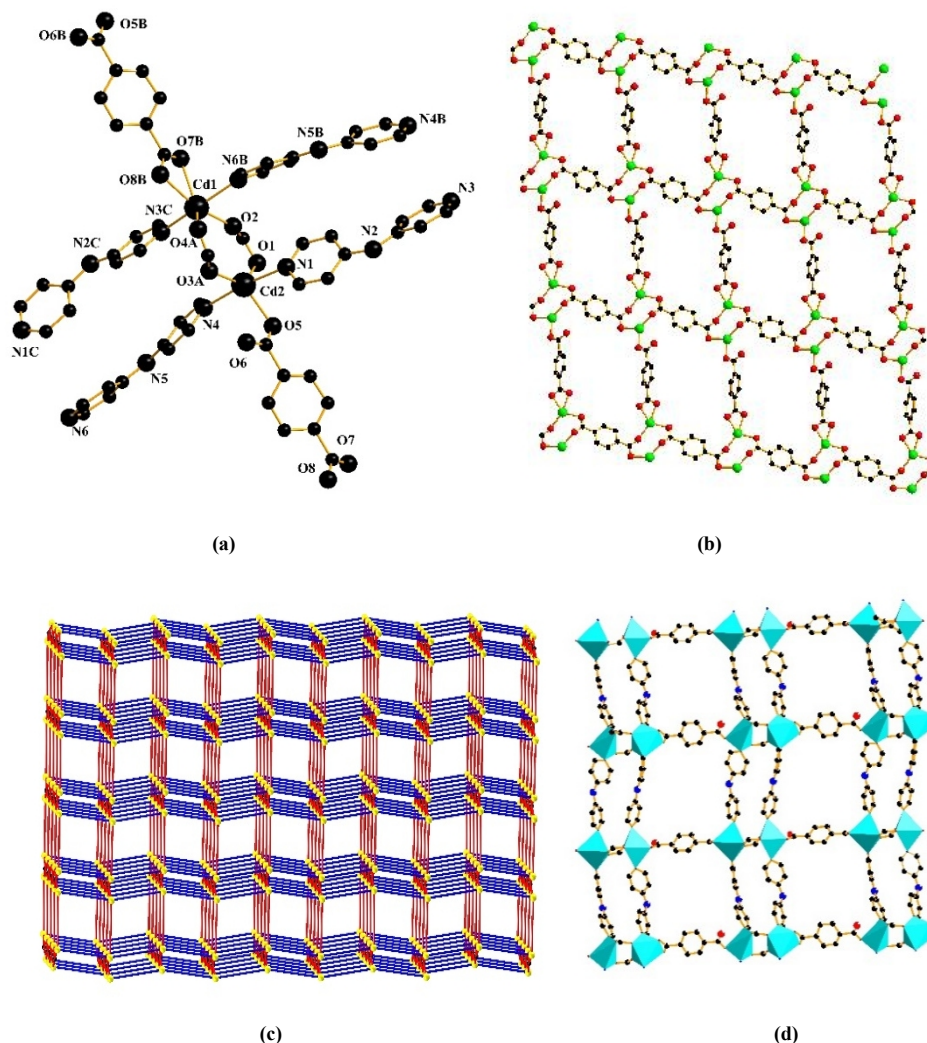


Fig. 1. (a) Coordination environment of Cd(II) in **1** (All hydrogens are omitted for clarity). (b) View of 2-D network in complex **1**. (c) Schematic representation of topology for complex **1**. (d) View of the 3-D framework for complex **1**

### 3.2 Crystal structure of

#### $\{[\text{Cd}(p\text{-BDC})(4,4'\text{-dpa})(\text{H}_2\text{O})]\cdot 4\text{H}_2\text{O}\}_n \mathbf{2}$

The single-crystal X-ray diffraction analysis reveals that complex **2** crystallizes in orthorhombic space group *Pbca*. The asymmetric unit of **2** contains one crystallographically unique Cd(II) ion, one *p*-BDC<sup>2-</sup> anion, one 4,4'-dpa ligand, one coordinated water molecule, and four lattice water molecules, as shown in Fig. 2. The Cd(II) ion is seven-coordinated in a pentagonal bipyramidal geometry by four oxygen atoms from two *p*-BDC<sup>2-</sup> anions, two nitrogen atoms of

4,4'-dpa ligands, and one oxygen from one coordinated water molecule. The Cd(1)–O bond lengths vary from 2.266(2) to 2.579(2) Å, and the Cd(1)–N bond lengths change from 2.3032(3) to 2.364(3) Å. In complex **2**, two different carboxylate groups adopt bidentate chelate coordination modes, which connect Cd(II) ions to form a 3-D structure. As shown in Fig. 3, from the perspective of topology, *p*-BDC<sup>2-</sup> and 4,4'-dpa as linkers connect two adjacent Cd metal atoms, so the structure of **2** could be simplified as a uninodal 4-connected net with a point symbol of (6<sup>6</sup>).

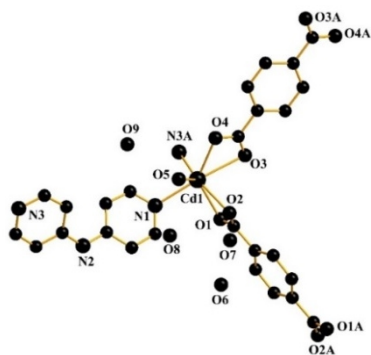


Fig. 2. Coordination environment for Cd(II) in complex 2 (All hydrogens have been omitted for clarity)

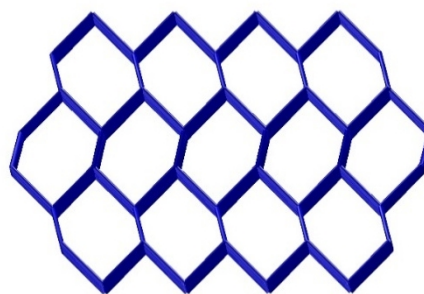


Fig. 3. Schematic representation of topology for complex 2

### 3.3 Hirshfeld surface analysis for complex 2

Hirshfeld surface analysis is an effective tool for the quantitative study of intermolecular interactions within crystal packings, which provides visual images of intercontacts and molecular shapes in a crystalline material. The Hirshfeld surfaces are mapped via the normalized contact distance ( $d_{\text{norm}}$ ) relative to both  $d_e$  and  $d_i$  and the van der Waals radius of the atoms, where  $d_e$  is the distance from a point on the surface to the nearest nucleus outside the surface and  $d_i$  is distance from a point on the surface to the nearest nucleus inside the surface<sup>[18]</sup>. The molecular Hirshfeld surface ( $d_{\text{norm}}$ ) of the complex can be used to show short intermolecular interactions (Fig. 4). The Hirshfeld surfaces mapped with  $d_{\text{norm}}$  and full fingerprint plots were made using CrystalExplorer software (Version 3.1). The  $d_{\text{norm}}$  value is negative (red) when intermolecular contacts are shorter than the van der Waals radii, and the  $d_{\text{norm}}$  (blue) when longer. The  $d_{\text{norm}}$  value of the white zone is zero and represents contacts equal to the van der Waals radius. The red spots in the picture are mainly caused by the hydrogen bonding between the carboxyl groups of the main ligand *p*-phthalic acid and free water molecules through  $\text{O}-\text{H}\cdots\text{O}$ . In this study, the  $d_{\text{norm}}$  values range from  $-1.188$  to  $1.429$  Å.

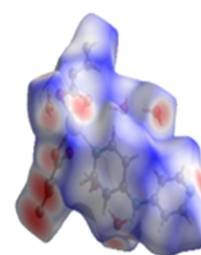


Fig. 4. Hirshfeld surfaces mapped with the  $d_{\text{norm}}$  function for 2

Each 2D fingerprint plot can be split into the respective close contacts, and their contributions can be expressed as percentages. The relative contributions of various interactions for **2** are presented in Fig. 5. The 2D fingerprint plots (Fig. 6) present contacts between two atoms interacting with each other and indicate percentage of contributions from different interaction types. The proportions of  $\text{H}\cdots\text{H}$  and  $\text{C}\cdots\text{H}$  are 40.8% and 5% respectively, while that of  $\text{O}\cdots\text{H}$  is 14%. In the interaction of molecules,  $\text{H}\cdots\text{H}$  and  $\text{O}\cdots\text{H}$  account for a large proportion, so van der Waals forces and hydrogen bonds play a significant role in the three-dimensional stacking structure, of which  $\text{O}-\text{H}\cdots\text{O}$  plays a major role in intermolecular hydrogen bonds. This corresponds to the fact the majority of the surface of this molecular crystal is covered with atoms of H.

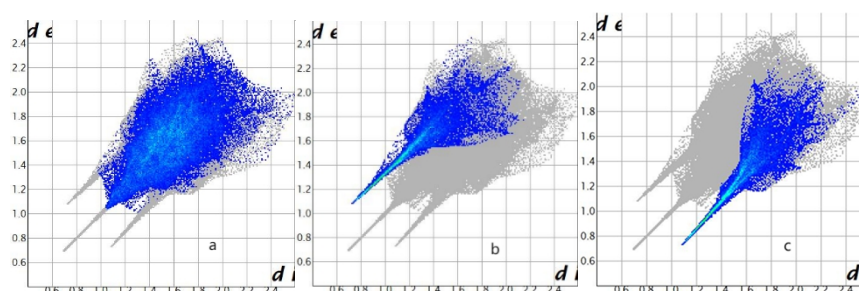


Fig. 5. Fingerprint plots for  $\text{H}\cdots\text{H}$  (a),  $\text{H}\cdots\text{O}$  (b) and  $\text{O}\cdots\text{H}$  (c) contacts of 2

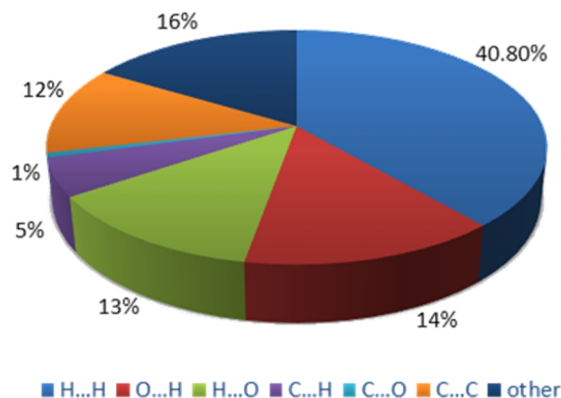


Fig. 6. Hirshfeld surface calculations for 2

### 3.4 Powder X-ray diffraction analysis

The powder X-ray diffraction (PXRD) patterns for the coordination polymers were recorded to investigate the crystalline phases of the polycrystalline materials. The

simulated and experimental PXRD patterns are shown in Fig. 7. Most of the PXRD peak positions in the simulated and experimental patterns are in good agreement with each other, indicating the pure samples of complexes **1** and **2**.

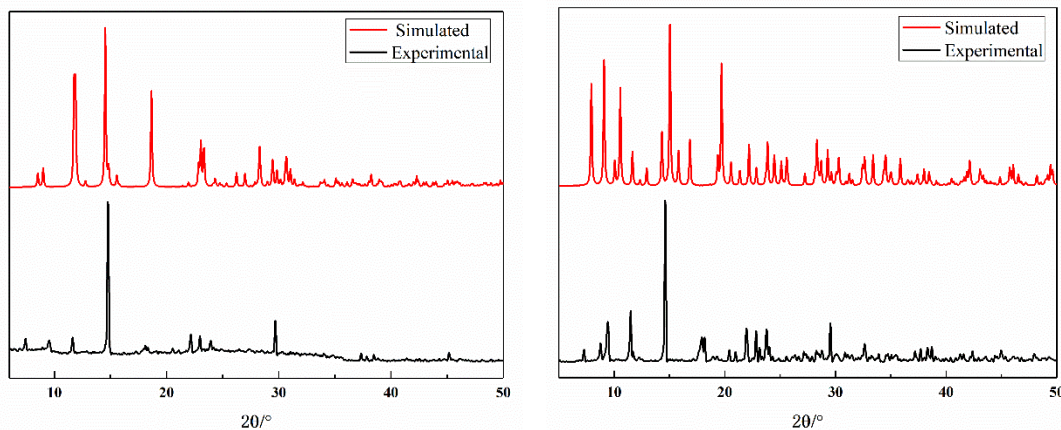


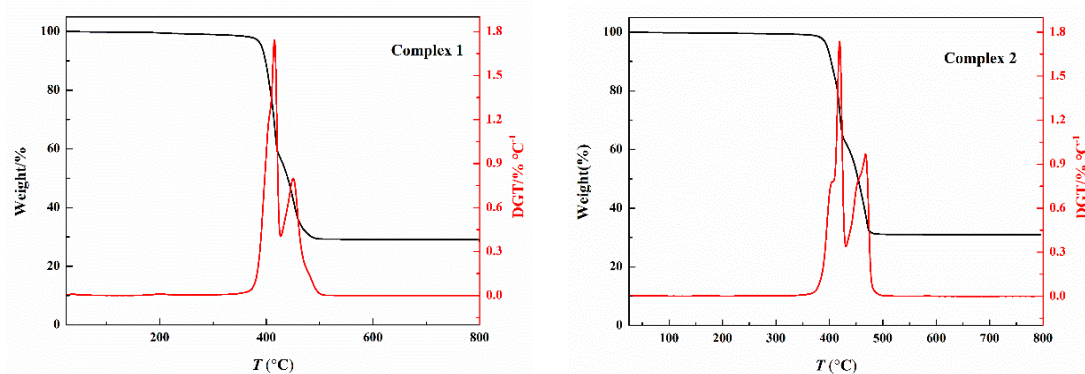
Fig. 7. XRD patterns of complexes 1 and 2

### 3.5 Thermal gravimetry analysis

To estimate the stabilities of the complexes, thermogravimetric (TG) analyses of complexes **1** and **2** were carried out under a N<sub>2</sub> atmosphere from 15 to 800 °C. The weight loss curves of complexes **1** and **2** are shown in Fig. 8. For **1**, the first stage 36.74% weight loss in the range of 379~417 °C is contributed to the decomposition of *p*-BDC<sup>2-</sup> ligands (calcd.: 37.10%). The second stage of 37.83% weight loss between 417 and 499 °C could be attributed to the departure of

4,4'-dpa ligands (calcd.: 38.19%). Above 500 °C, the curve area is stable, and the final mass remnant is likely consistent with the deposition of CdO. For **2**, the first stage 30.59% weight loss in the range of 385~422 °C results from the decomposition of *p*-BDC<sup>2-</sup> ligand (calcd.: 30.91%). The second stage of 32.01% weight loss between 422 and 473 °C is assigned to the removal of 4,4'-dpa ligand (calcd.: 31.81%). When reaching 500 °C, the curve area is stable, and the final mass remnant is likely consistent with the deposition of CdO.

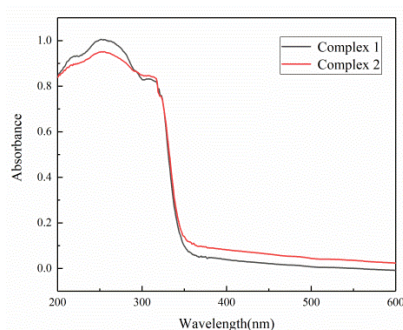
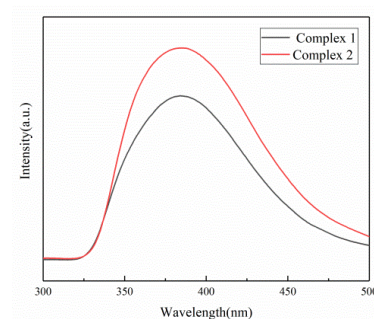


Fig. 8. Thermal behaviours of **1** and **2**

### 3.6 Luminescent properties

The solid state UV-vis absorption of complexes **1** and **2** was measured (Fig. 9). The maximum absorption peaks are all around 270 nm. It is well known that coordination polymers constructed by  $d^{10}$  metal center and conjugated organic linkers are promising candidates for photoactive materials, with potential applications such as chemical sensors and in photochemistry<sup>[19-22]</sup>. Considering the excellent luminescent properties of  $d^{10}$  transition metal-organic polymers<sup>[23, 24]</sup>, the solid-state photoluminescent properties of complexes **1** and **2** were investigated at room

temperature. All bands can be assigned to the intraligand  $\pi^* \rightarrow \pi$  or  $\pi^* \rightarrow n$  emission<sup>[25]</sup>. Since the Cd(II) ions are difficult to oxidize or reduce, the emission of complex **1** and **2** is neither metal-to-ligand charge transfer (MLCT) nor ligand-to-metal charge transfer (LMCT)<sup>[26]</sup>. As shown in Fig. 10, complex **1** exhibits the maximum emission at 385 nm ( $\lambda_{\text{ex}} = 270$  nm), and complex **2** shows the maximum emission at 385 nm ( $\lambda_{\text{ex}} = 270$  nm). Compared with **2**, the luminous intensity of complex **1** is reduced. The emission discrepancy of **1** and **2** is probably due to the differences of coordination environments of the central metal ions<sup>[27-29]</sup>.

Fig. 9. Solid-state UV-vis absorption spectra of complexes **1** and **2**Fig. 10. Emission spectra of complexes **1** and **2** in the solid state at room temperature

## 4 CONCLUSION

In this paper, we have synthesized two Cd(II) coordination polymers whose structures and properties were different because of the different temperature. Remarkably, the changes in coordination numbers of metal atoms and coordination modes stimulated by reaction temperature result in

the distinct frameworks of **1** and **2**, which promote us to make a further research on related functional crystalline solids through such a reliable synthetic procedure. This work demonstrates that the temperature has a significant effect on the structures and properties of coordination polymers. The luminescent properties of complexes **1** and **2** imply that they may be good candidates for luminescent materials.

## DISCLOSURE STATEMENT

No potential conflict of interest was reported by the authors.

## REFERENCES

- (1) He, Z. W.; Liu, C. J.; Li, W. D.; Han, S. S.; Chen, S. S. Two interpenetrated Zn(II) coordination polymers: synthesis, topological structures, and property. *Crystals* **2019**, 9, 601–608.
- (2) Zhu, Q.; Sheng, T.; Fu, R.; Hu, S.; Shen, C.; Ma, X.; Wu, X. Syntheses, structural aspects, luminescence and magnetism of four coordination polymers based on a new flexible polycarboxylate. *Crystengcomm.* **2011**, 13, 2096–2105.
- (3) Gai, Y. L.; Zhao, X. Y.; Chen, Y.; Liang, B.; Li, X.; Guo, X. Y.; Huang, Q.; Liu, L. J.; Xiong, K. C. Syntheses, characterization, and fluorescence properties of four coordination polymers based on double betaine ligands. *Z. Anorg. Allg. Chem.* **2018**, 644, 397–404.
- (4) Gao, L.; Bian, Y.; Tian, Y.; Chen, Y.; Hu, T. Structural diversity, gas adsorption and magnetic properties of three coordination polymers based on a rigid multicarboxylate ligand. *CrystEngComm.* **2020**, 22, 7046–7053.
- (5) Yin, G. J.; Zhang, H. Y.; Tian, W. J.; Zhao, D.; Zhang, B.; Chen, D. M. Synthesis and optical property of a new zinc complex based on the derivative of 2-(2'-hydroxyphenyl)-1H-benzimidazole and phenanthroline. *Chin. J. Struct. Chem.* **2021**, 40, 487–494.
- (6) Si, C. D.; Hu, D. C.; Fan, Y.; Wu, Y.; Yao, X. Q.; Yang, Y. X.; Liu, J. C. Seven coordination polymers derived from semirigid tetracarboxylic acids and N-donor ligands: topological structures, unusual magnetic properties, and photoluminescences. *Cryst. Growth Des.* **2015**, 15, 2419–2432.
- (7) Lin, L.; Chen, Y. F.; Qiu, L. J.; Zhu, B.; Wang, X.; Luo, S. P.; Shi, W.; Yang, T. H.; Lei, W. Synthesis, structure and photocatalytic properties of coordination polymers based on pyrazole carboxylic acid ligands. *CrystEngComm.* **2020**, 22, 6612–6619.
- (8) Abbasi, A. R.; Yousefshahi, M.; Daasbjerg, K. Non-enzymatic electroanalytical sensing of glucose based on nano nickel-coordination polymers-modified glassy carbon electrode. *J. Inorg. Organomet. Polym.* **2020**, 30, 2027–2038.
- (9) Hanna, K.; Daniel, L.; Ingmar, P. Solvation and coordination chemistry of manganese(II) in some solvents. A transfer thermodynamic, complex formation, EXAFS spectroscopic and crystallographic study. *Polyhedron* **2020**, 195, 114961–114969.
- (10) Yang, G. P.; Hou, L.; Ma, L. F.; Wang, Y. Y. Investigation on the prime factors influencing the formation of entangled metal-organic frameworks. *CrystEngComm.* **2013**, 15, 2561–2578.
- (11) Zhang, D. M.; Xu, C. G.; Liu, Y. Z.; Fan, C. B.; Fan, Y. H. A series of coordination polymers based on 2,6-pyridinedicarboxylic acid ligand: synthesis, crystal structures, photo-catalysis and fluorescent sensing. *J. Solid State Chem.* **2020**, 290, 121549–121560.
- (12) Chen, M.; Lu, Y.; Fan, J.; Lv, G. C.; Zhao, Y.; Zhang, Y.; Sun, W. Y. High structural diversity controlled by temperature and induction agent. *CrystEngComm.* **2012**, 14, 2015–2023.
- (13) Bruker, APEX2 (Version1.08). SAINT (Version7.03), SADABS (Version2.11), SHELXTL (Version 6.12), Bruker AXS Inc, Madison, WI, USA **2004**.
- (14) Sheldrick, G. M. A short history of SHELX. Section A: foundations of crystallography. *ActaCrystallogr.* **2008**, 64, 112–122.
- (15) Sheldrick, G. M. *SHELXS-97. Program for Crystal Structure Solution*. University of Gottingen, Germany **1997**.
- (16) Sheldrick, G. M. *SHELXL-97. Program for Crystal Structure Refinement*. University of Gottingen, Germany **1997**.
- (17) Yu, Q.; Zhang, X. Q.; Deng, J. H.; Bian, H. D.; Liang, H. Aqua-bis(1-formyl-2-naphtholato- $\kappa^2$ O,O')copper(II). *ActaCrystallogr.* **2006**, 62, m391–m393.
- (18) Martin, A. D.; Britton, J.; Easun, T. L.; Blake, A. J.; Lewis, W.; Schröder, M. Hirshfeld surface investigation of structure-directing interactions within dipicolinic acid derivatives. *Cryst. Growth Des.* **2015**, 15, 1697–1706.
- (19) Fu, M. M.; Qu, Y. H.; Blatov, V. A.; Li, Y. H.; Cui, G. H. Two  $d_{10}$  metal coordination polymers as dual functional luminescent probes for sensing of  $\text{Fe}^{3+}$  ions and acetylacetone with high selectivity and sensitivity. *J. Solid State Chem.* **2020**, 289, 121460–121469.
- (20) Chen, S. S.; Han, S. S.; Ma, C. B.; Li, W. D.; Zhao, Y. A series of metal-organic frameworks: syntheses, structures and luminescent detection, gas adsorption, magnetic properties. *Cryst. Growth Des.* **2021**, 21, 869–885.
- (21) Luo, G. G.; Xiong, H. B.; Sun, D.; Dong, L. W.; Rong, B. H.; Jing, C. D. A discrete spirocyclic  $(\text{H}_2\text{O})_9$  cluster and 1D novel water chain with tetrameric and octameric clusters in cationic hosts. *Cryst. Growth Des.* **2011**, 11, 1948–1956.
- (22) Dovgaliuk, I.; Nouar, F.; Serre, C.; Filinchuk, F.; Chernyshov, D. Cooperative adsorption by porous frameworks: diffraction experiment and phenomenological theory. *Chem-Eur. J.* **2017**, 23, 17714–17720.
- (23) Kan, W. Q.; Zhang, Z. C.; He, Y. C.; Wen, S. Z.; Zhao, P. S. Syntheses, crystal structures, characterization, optical band gaps and photoluminescence of two Zn(II) coordination polymers. *J. Chem Crystallogr.* **2020**, 51, 42–49.
- (24) Wang, Y. T.; Tang, G. M.; Wang, C. C. Two  $d_{10}$  metal-organic frameworks based on a novel semi-rigid aromatic biscarboxylate ligand: syntheses, structures and luminescent properties. *Appl. Organomet. Chem.* **2020**, 34, e56541–e565412.
- (25) Zhao, H. Y.; Yang, F. L.; Li, N.; Wang, X. J. Halide/pseudohalide complexes of cadmium(II) with benzimidazole: synthesis, crystal structures and



- fluorescence properties. *J. Mol. Struct.* **2017**, 1148, 62–72.
- (26) Wei, L. L.; Li, L. K.; Fan, L. Y.; Wang, C. H.; Hou, H. W. Crystal structures, and properties of six coordination complexes based on a newly designed mercapto-thiadiazole ligand. *Aust. J. Chem.* **2014**, 67, 241–249.
- (27) Deng, D. S.; Kang, G. H.; Ji, B. M.; Li, H. L.; Qu, G. R.; Fan, X. S.; Ruan, C. S.; Li, T. S.; Wang, M. C. Syntheses, photoluminescent properties, and structural investigation of five complexes based on a new T-shaped 2-(pyridin-3-yl)-4,6-pyrimidine dicarboxylic acid ligand: structure evolution from one-dimensional chains to three-dimensional architectures. *Aust. J. Chem.* **2013**, 66, 1342–1351.
- (28) Wen, L. L.; Dang, D. B.; Duan, C. Y.; Li, Y. Z.; Tian, Z. F. Meng, Q. J. 1D helix, 2D brick-wall and herringbone, and 3D interpenetration  $d_{10}$  metal-organic framework structures assembled from pyridine-2,6-dicarboxylic acid N-oxide. *Inorg. Chem.* **2005**, 44, 7161–7170.
- (29) Liu, L.; Huang, C.; Wang, Z.; Wu, D.; Hou, H.; Fan, Y. Entangled Zn(II)/Cd(II) coordination complexes based on a flexible bis(methylbenzimidazole) ligand and different dicarboxylates. *CrystEngComm.* **2013**, 15, 7095–7105.